

eAppendix Methods 1: ICD-9 codes of diagnoses

The diagnoses are classified using ICD-9 codes and are primary discharge causes of hospital admissions. Cardiovascular diseases are coded as the sum of admissions for ICD-9 390 to 459, including heart failure (ICD-9 428), heart rhythm disturbances (ICD-9 426–427), cerebrovascular events (ICD-9 430–438), ischemic heart disease (ICD-9 410–414 and 429), and peripheral vascular disease (ICD-9 440–449). Respiratory diseases are the aggregated admissions for chronic obstructive pulmonary disease (COPD) (ICD-9 490–492) and respiratory tract infections (ICD-9 464–466, 480–487).

eAppendix Methods 2: details on GEOS-Chem modeling

GEOS-Chem is a 3-dimensional global chemistry model that solves for the temporal and spatial evolution of gas-phase species and aerosol (<http://acmg.seas.harvard.edu/geos/index.html>). Input to the model consists of gridded meteorological data sets at fine spatial and temporal resolution as well as both anthropogenic and wildfire emission inventories. Here we use meteorological fields from the Goddard Earth Observing System (GEOS-5) of the NASA Modeling and Assimilation Office (GMAO). We also apply observed wildfire area burned based on the Global Fire Emissions Database (GFED3), a resource heavily relied on by the atmospheric community (<http://www.globalfiredata.org>). Given these input fields, GEOS-Chem calculates the chemistry, transport, and fate of atmospheric species, using equations that represent the physics and chemistry of atmospheric composition. For this study, we used the aerosol-only version of GEOS-Chem, which includes emissions of all primary particulate matter as well as the gas-phase precursors to secondary particulate matter. Oxidation of gas-phase precursors in this version of the model is carried out through application of monthly mean fields of oxidants calculated beforehand with the full-chemistry version of GEOS-Chem. Output from GEOS-Chem consists of 3-dimensional gridded output of speciated, daily mean particulate matter in terms of mass. Total $PM_{2.5}$ in the model is taken to be the sum of sulfate, nitrate, ammonium, organic carbon and black carbon. We identify wildfire-specific $PM_{2.5}$ by performing a pair of simulations – one with fire emissions turned on and one without these emissions. Wildfire-specific $PM_{2.5}$ is defined as the difference in $PM_{2.5}$ output from these two simulations.

GEOS-Chem concentrations of $PM_{2.5}$ over the United States, including wildfire $PM_{2.5}$, have been extensively validated on a variety of timescales, including daily³⁻⁶ and seasonal⁷. Zhang et al. (2014)⁸, while focused on ozone, included validation of daily mean wildfire $PM_{2.5}$ in GEOS-Chem. Simulated wildfire $PM_{2.5}$ from other regions has also been evaluated on daily timescales (e.g. ^{9,10}). We use

ground-based or aircraft measurements, not satellite data, to validate the GEOS-Chem surface $PM_{2.5}$, including wildfire $PM_{2.5}$. Satellite data of particulate matter are not useful to validate surface $PM_{2.5}$ mainly because such data describe the *column amount* of particulate matter through the atmosphere in $mg\ m^{-2}$, not the *surface* concentrations in $\mu g\ m^{-3}$. Efforts have been made to infer surface concentrations of $PM_{2.5}$ from satellite data, but such efforts rely, in fact, on GEOS-Chem to translate column amounts into surface levels (e.g., ¹¹).

GEOS-Chem has been used previously to assess the health impacts of surface pollution. For example, van Donkelaar et al. (2015)¹¹ used GEOS-Chem simulations to convert satellite observations of column particulate matter (in $mg\ m^{-2}$) into surface concentrations (in $\mu g\ m^{-3}$). This study calculated 2001-2012 global trends in annual mean $PM_{2.5}$ at the surface at $\sim 10 \times 10$ km, the spatial resolution of the satellite data. The GEOS-Chem simulation for van Donkelaar et al. (2015) was performed at 2×2.5 degree resolution globally ($\sim 200 \times 250$ km), with a few target regions at 0.5×0.67 degrees, the same resolution as we used here for the western United States. The van Donkelaar et al. (2015) approach cannot distinguish between wildfire $PM_{2.5}$ and other types of particulate matter and achieves fine spatial resolution only at the expense of temporal resolution. (The satellite data at 10×10 km spatial scales are noisy on the daily level.) Our use of GEOS-Chem takes advantage of the model's capability to fill in the temporal and spatial gaps in the ground-based network and allows us to diagnose wildfire-specific $PM_{2.5}$ at the daily level.

eAppendix Methods 3: Details about area weighted averaging

We added a gridded layer (0.5×0.67 degree) on top of an equal-area projected map of the study domain (31-49N, 101-125W). There are 1332 grids in the study domain, 1188 of which overlapped with the Western US boundary. We calculated the areas of each county and each fragment the grids fall in the counties. Then we calculated the area ratio of each grid fragment within a county's boundary by dividing county area by fragment area. The county-level exposure was the sum of each area ratio in the county times the concentration in the grids that fall into the county.

eAppendix Methods 4: Statistical Modeling

We fitted a log-linear mixed-effects regression model for each disease group (cardiovascular or respiratory diseases) for smoke wave days and matched control days across all 561 counties. The model can be expressed as:

$$\log E(Y_t^c) = \log(n_t^c) + \alpha + a^c + \beta SW_t^c + \delta_1 tmpd + \delta_2 PMamb + \delta_3 \sum_{j=1}^3 agecat^c + \delta_4 \sum_{k=1}^2 gender^c + \delta_5 \sum_{l=1}^3 race^c + \delta_6 \sum_{m=1}^2 weekend + \delta_7 \sum_{n=1}^6 year$$

Where:

Y_t^c is the count of hospital admissions for a disease group on day t in county c . We assume Y follows a Poisson distribution.

n_t^c is the total population at risk on day t in county c .

a^c is county-specific random effect.

SW_t^c is a binary indicator for smoke wave day or non-smoke-wave day.

We adjusted for scaled temperature ($tmpd$), modeled non-fire $PM_{2.5}$ levels ($PMamb$), age categories ($agecat$: 65-74, 75-84, 85+ years), gender categories, race categories (White, Black, other), weekend or weekday, and study year. A binary indicator variable for smoke wave was specified as 1 on a smoke wave day and 0 on matched non-smoke-wave days. The model included a county-specific random intercept and fixed effect for daily continuous measurement of temperature, modeled non-fire $PM_{2.5}$ levels, sex (male, female), age category (65-74, 75-84, $\geq 85y$), race (White, Black, other), type of day (weekend, weekday), and year. The analysis is weighted, which means smoke wave days matched with <3 non-smoke-wave days are weighted less than smoke wave days matched with three non-smoke-wave days. This model estimates the relative rate (RR) of hospital admissions on smoke wave days compared with non-smoke-wave days.

eAppendix Results 1: Single-day smoke wave results

The sensitivity analysis of the association between single-day smoke wave and hospital admissions showed stronger effect than the effect of the smoke wave days using main definition (≥ 2 consecutive days with wildfire-specific $PM_{2.5} > 20 \mu g/m^3$) (Table A.4). Compared to matched control days with wildfire-specific $PM_{2.5} \leq 20 \mu g/m^3$, single-day smoke waves (daily_wildfire-specific $PM_{2.5} > 20 \mu g/m^3$) are associated with an increase of 5.65% (95% CI: 1.23%, 10.26%) in respiratory hospital admissions. The trend of effect by smoke wave intensity is consistent with that of the main analysis, i.e. more intense smoke waves led to higher associations. No association was observed between single-day smoke waves and CVD admissions. Single-day smoke waves have potentially stronger association with respiratory admissions rate, possibly due to a larger sample size and the acute response of respiratory diseases.

eAppendix Results 2: Smoke wave effect among counties with fee-for-service enrollment $\geq 75\%$

Our study populations are Medicare beneficiaries who are enrolled in the fee-for-service plan. Counties have different percentage of Medicare beneficiaries enrolled in the fee-for-service plan. Average percentage of fee-for-service enrollment in a county is 89.4% among the 561 counties. Of the 561 counties, 471 (84%) had over 80% Medicare beneficiaries enrolled in the fee-for-service plan. Only 30 out of the 561 counties (5%) had <60% FFS coverage.

To examine whether the differences in fee-for-service enrollment leads to selection bias, we conducted sensitivity analysis among counties with fee-for-service enrollment $\geq 75\%$ for intense smoke wave days (with wildfire-specific $PM_{2.5}$ threshold = $37\mu g/m^3$). There are 176 counties that experience at least one intense smoke wave and with fee-for-service enrollment $\geq 75\%$. Compared to matched control days with wildfire-specific $PM_{2.5} \leq 20\mu g/m^3$, the effect of intense smoke wave days on respiratory admissions is: 7.4% (95% CI: -6.3%, 23.2%).

eTable 1. Selected quantile values in original modeled total $PM_{2.5}$, monitoring $PM_{2.5}$, and calibrated modeled total $PM_{2.5}$ ($\mu g/m^3$).

% quantiles	0	10	20	30	40	50	60	70	80	90	100
Original modeled total PM	0.02	1.14	1.61	2.02	2.44	2.90	3.43	4.10	5.12	7.28	2902.4
Monitoring PM	0	3.65	4.73	5.70	6.60	7.60	8.70	10.20	12.23	15.70	242.58
Calibrated modeled total PM	0	3.65	4.73	5.70	6.60	7.60	8.70	10.20	12.23	15.70	242.58

eTable 2. Frequency distribution and average temperature of smoke wave county-days and matched non-smoke-wave county-days in different years.

Smoke wave days								
	May	June	July	August	September	October	Total (% among all smoke wave days)	Average Temperature (°F)
2004	7	5	144	305	28	112	601 (5.96)	67.7
2005	0	40	34	453	123	1	651 (6.46)	68.6
2006	0	87	279	958	1200	28	2552 (25.3)	70.5
2007	0	29	724	1554	430	47	2784 (27.6)	68.7
2008	6	543	1882	323	246	51	3051 (30.3)	67.1
2009	0	0	46	245	150	0	441 (4.38)	68.6
Total (% among all smoke wave days)	13 (0.13)	704 (6.98)	3109 (30.8)	3838 (38.1)	2177 (21.6)	239 (2.37)	10,080 (100)	68.5
Matched Non-smoke-wave days								
	May	June	July	August	September	October	Total (% among all matched non-smoke-wave days)	Average Temperature (°F)
2004	5	416	1901	2163	1226	116	5827 (20.0)	71.6
2005	9	362	1912	1877	1197	145	5502 (18.9)	67.4
2006	8	352	1659	1368	453	118	3958 (13.6)	68.1
2007	6	356	1371	1087	828	169	3817 (13.1)	70.7
2008	7	152	753	2010	1011	127	4060 (13.9)	70.4
2009	9	422	1963	2204	1210	173	5981 (20.5)	72.3
Total (% among all matched non-smoke-wave days)	44 (0.15)	2060 (7.07)	9559 (32.8)	10709 (36.7)	5925 (20.3)	848 (2.91)	29,145 (100)	69.9

eTable 3 (a). Average daily surface temperature during smoke wave days with different intensities of smoke wave days (daily wildfire-specific PM_{2.5} levels). “smokewave₉₈” denotes smoke wave days defined with a threshold of 98th percentile of all daily wildfire-specific PM_{2.5} values in all counties.

Intensity of smokewave ₉₈ days (µg/m ³)	Temperature (°F)
20-23 (98 th – 98.5 th quantile)	70.0
23.01-28 (98.5 th – 99 th quantile)	70.3
28.01-37 (99 th – 99.5 th quantile)	70.1
>37 (>99.5 th quantile)	69.3

eTable 3 (b). Average daily surface temperature during smoke wave days with different intensities of smoke wave days (daily wildfire-specific PM_{2.5} levels).

Length of smokewave ₂₀ (days)	Temperature (°F)
2 (20% quantile)	70.3
3 (40% quantile)	70.1
4-5 (60% quantile)	71.9
6+ (80% quantile)	69.0

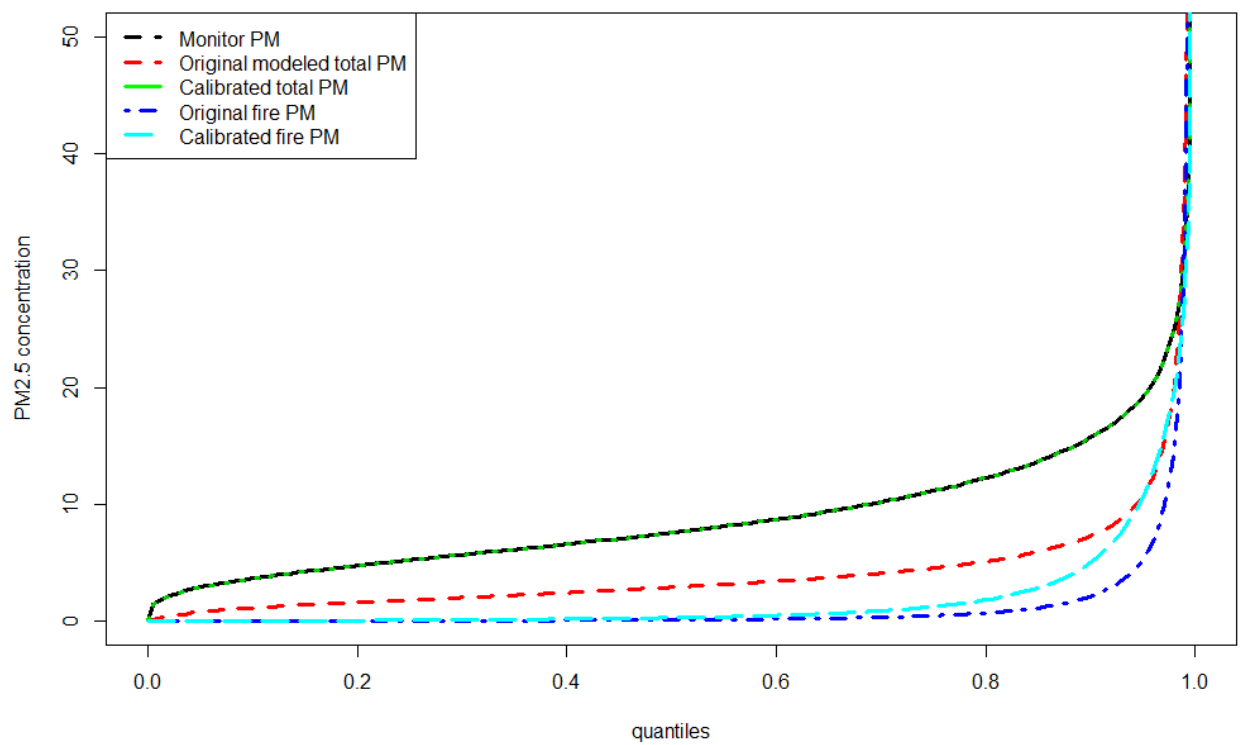
eTable 4. Results of sensitivity analysis: association between single-day smoke waves and CVD and respiratory admissions for the study population during 2004-2009*.

Threshold (µg/m ³)	CVD effect (95% CI)	Respiratory effect (95% CI)
20	-0.31 (-1.95, 2.62)	5.65 (1.23, 10.26)
23	-0.14 (-2.60, 2.38)	6.08 (1.23, 11.17)
28	0.36 (-2.44, 3.23)	8.27 (2.68, 14.15)
37	-1.22 (-4.66, 2.35)	11.20 (4.07, 18.82)

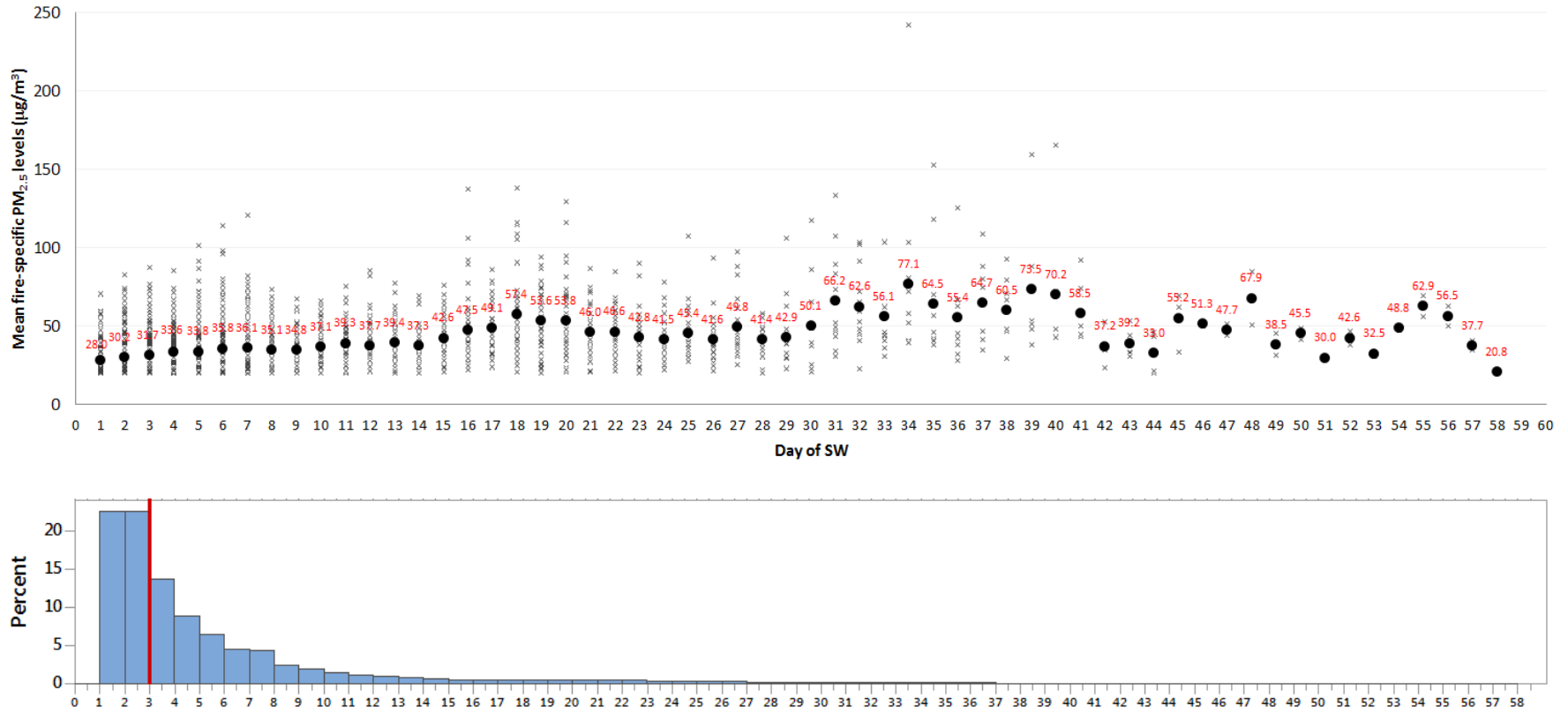
*Significant results are denoted in bold.



eFigure 1. Study domain.



eFigure 2. Quantile distribution plot for monitoring data, original modeled total PM_{2.5}, and calibrated total PM_{2.5}. After calibration the calibrated total PM_{2.5} now has similar mean and variance as real-world measurements.



eFigure 3. Wildfire-specific PM_{2.5} across all smoke wave days: a) Average daily wildfire-specific PM_{2.5} in each day within a smoke wave, b) frequency of smoke waves durations in days during 2004-2009. For the top panel, the solid black circles are the mean wildfire-PM_{2.5} levels on a given day within a smoke wave (e.g., 1 represents the first day of a smoke wave, 2 the second day of a smoke wave). The numbers in red are the mean wildfire-PM_{2.5} values for that day within a smoke wave (i.e., the red number represents the mean of the black circles for that day within a smoke wave). Each “x” represents the intensity of one smoke wave day in one county. The bottom panel shows the frequency of smoke wave days within a smoke wave. The red vertical line represents the median length of smoke waves.

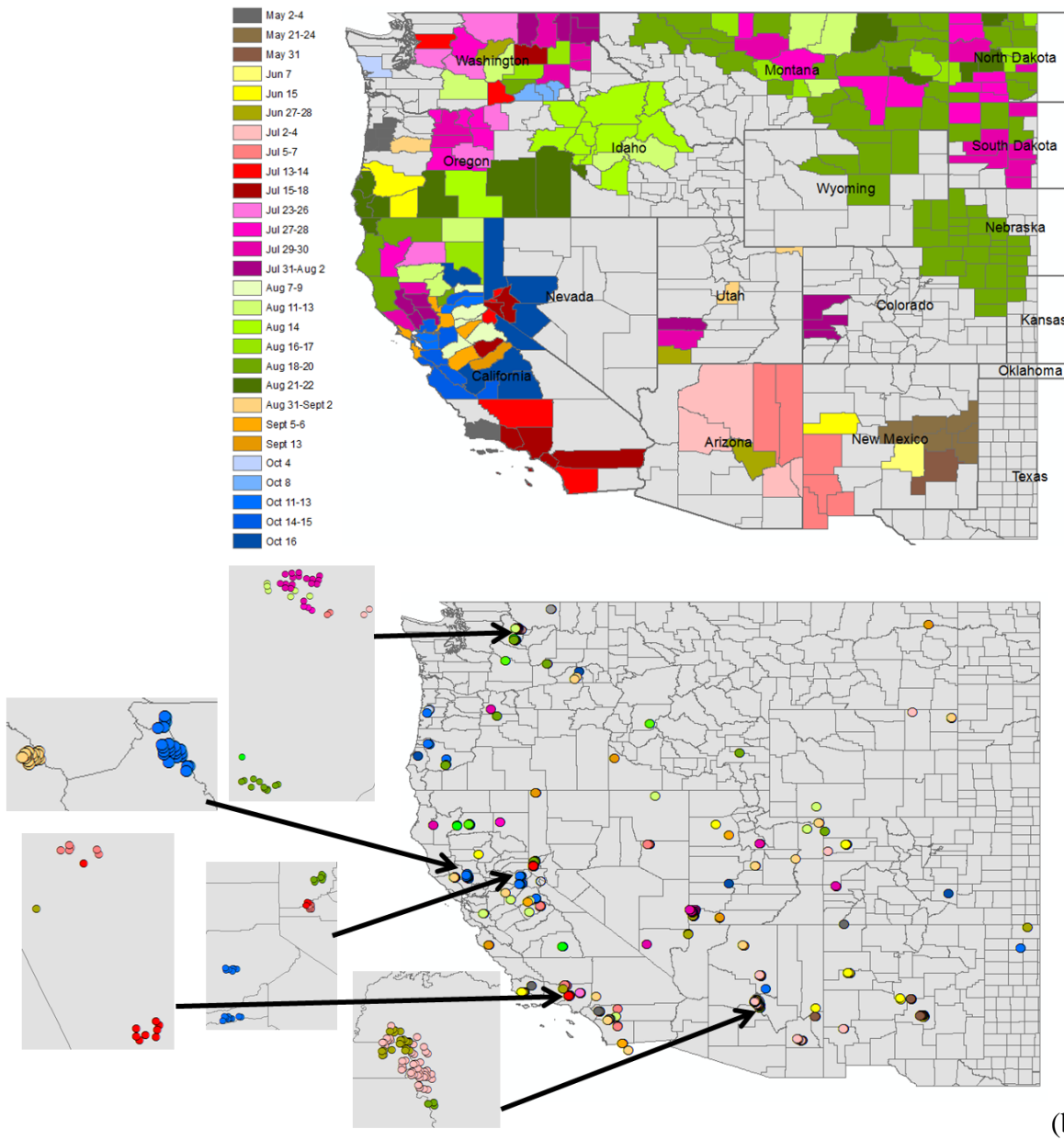


Figure 4. Dates and locations of smoke wave days (a) in 2004 compared with dates and locations of MODIS satellite records of large wildfire events in 2004 (fire radiative power >500)¹ (b). Each color represents a different range of 1-4 days. The same color in (a) and (b) indicates the same range of 1-4 days.

Since smoke wave days are defined based on daily wildfire-specific PM_{2.5} (rather than fire event days), their dates and locations do not necessarily reflect the exact dates and locations of wildfire events. We found that the dates and locations of smoke wave days generally matched well with MODIS records of large wildfires. The smoke wave days in North Dakota, South Dakota and Montana are due to wildfires in Canada as wildfire smoke can travel across continent².

References

1. USDA Forest Service Remote Sensing Applications Center (RSAC). 2004 MODIS MCD14ML Collection 5, Version 1 (CONUS). 2010.
2. Sapkota A, Symons JM, Kleissl J, Wang L, Parlange MB, Ondov J, Breysse PN, Diette GB, Eggleston PA, Buckley TJ. Impact of the 2002 Canadian forest fires on particulate matter air quality in Baltimore City. *Environmental Science & Technology* 2005;**39**(1):24-32.
3. Heald CL, Jacob DJ, Park RJ, Alexander B, Fairlie TD, Yantosca RM, Chu DA. Transpacific transport of Asian anthropogenic aerosols and its impact on surface air quality in the United States. *Journal of Geophysical Research-Atmospheres* 2006;**111**(D14).
4. Kim PS, Jacob DJ, Fisher JA, Travis K, Yu K, Zhu L, Yantosca RM, Sulprizio MP, Jimenez JL, Campuzano-Jost P, Froyd KD, Liao J, Hair JW, Fenn MA, Butler CF, Wagner NL, Gordon TD, Welti A, Wennberg PO, Crouse JD, St Clair JM, Teng AP, Millet DB, Schwarz JP, Markovic MZ, Perring AE. N Sources, seasonality, and trends of southeast US aerosol: an integrated analysis of surface, aircraft, and satellite observations with the GEOS-Chem chemical transport model. *Atmospheric Chemistry and Physics* 2015;**15**(18):10411-10433.
5. Li SS, Garay MJ, Chen LF, Rees E, Liu Y. Comparison of GEOS-Chem aerosol optical depth with AERONET and MISR data over the contiguous United States. *Journal of Geophysical Research-Atmospheres* 2013;**118**(19):11228-11241.
6. Park RJ, Jacob DJ, Kumar N, Yantosca RM. Regional visibility statistics in the United States: Natural and transboundary pollution influences, and implications for the Regional Haze Rule. *Atmospheric Environment* 2006;**40**(28):5405-5423.
7. Spracklen DV, Mickley LJ, Logan JA, Hudman RC, Yevich R, Flannigan MD, Westerling AL. Impacts of climate change from 2000 to 2050 on wildfire activity and carbonaceous aerosol concentrations in the western United States. *Journal of Geophysical Research-Atmospheres* 2009;**114**.
8. Zhang L, Jacob DJ, Yue X, Downey NV, Wood DA, Blewitt D. Sources contributing to background surface ozone in the US Intermountain West. *Atmospheric Chemistry and Physics* 2014;**14**(11):5295-5309.
9. Shen Z, Liu J, Horowitz LW, Henze DK, Fan S, Levy H, Mauzerall DL, Lin JT, Tao S. Analysis of transpacific transport of black carbon during HIPPO-3: implications for black carbon aging. *Atmospheric Chemistry and Physics* 2014;**14**(12):6315-6327.
10. Wang Q, Jacob DJ, Fisher JA, Mao J, Leibensperger EM, Carouge CC, Le Sager P, Kondo Y, Jimenez JL, Cubison MJ, Doherty SJ. Sources of carbonaceous aerosols and deposited black carbon in the Arctic in winter-spring: implications for radiative forcing. *Atmospheric Chemistry and Physics* 2011;**11**(23):12453-12473.
11. van Donkelaar A, Martin RV, Brauer M, Boys BL. Use of Satellite Observations for Long-Term Exposure Assessment of Global Concentrations of Fine Particulate Matter. *Environmental Health Perspectives* 2015;**123**(2):135-143.